Electronic Supplementary Material (ESI) for ChemComm.

Electronic Supplementary Information

Polymorphism of metal-organic frameworks: Direct comparison of structures and theoretical N_2-uptake of topological *pto*- and *tbo*- isomers

Nianyong Zhu, Matthew J. Lennox, Tina Düren and Wolfgang Schmitt*

A. Synthesis

1,3,5-Benzene-tris-ethynylbenzoic acid (BTEB) was synthesized as described by R. K. Castellano and J. Rebek, Jr., *J. Am. Chem. Soc.*, **1998**, *120*, 3657. Solvents, 4,4'-bipyridine and $Cu(NO_3)_2.3H_2O$ were used as purchased.

Preparation of $[Cu_3(BTEB)_2(H_2O)_3]$, TCM-4':

0.035 g BTEB (0.069 mmol) were added to a blue solution of 0.50 ml DMF containing 0.0163g $Cu(NO_3)_2.3H_2O$ (0.068 mmol). The resulting solution was sonicated for 10 minutes, and then 0.011g 4,4'-bipyridine (0.070 mmol) in 0.125 ml DMF and 0.50 ml DMF were added. The reaction mixture was heated in a closed vial at 85°C in oven for 48h. Blue, elongated, plate-like crystals were obtained. Yield: *ca.* 65%; Elemental analysis (%) of a dried sample of **TCM-4'** ($[C_{66}H_{36}Cu_3O_{15}].3H_2O$); found: C 60.12, H 2.32, N 0.00; calcd: C 60.34, H 3.22, N 0.00. FT-IR spectrum of the dried sample is shown in Fig. S1.

Preparation of $[Cu_3(BTEB)_2(H_2O)_3]$, TCM-8:

0.024 g BTEB (0.047 mmol) were added to a blue solution of 1.0 ml DMF containing 0.0167 g $Cu(NO_3)_2.3H_2O$ (0.069 mmol). The resulting solution was sonicated for 10 minutes. After that, the reaction solution was transferred into a closed 1.5 ml glass vial and heated in an oven at 85˚C for 24h. After cooling to room temperature, light blue crystals of **TCM-8** were collected, washed with DMF several times and stored in DMF. Yield *ca.* 85%; Elemental analysis (%) of a dried sample of **TCM-8** ($[C_{66}H_{36}Cu_3O_{15}].3H_2O$); found: C 60.03, H 2.65, N 0.00; calcd: C 60.34, H 3.20, N 0.00. The FT-IR spectrum of the dried sample is almost identical to that of **TCM-4'** and is shown in Fig. S1. Samples for CHN and FT-IR analysis were de-solvated and dried using solvent-exchange procedures using dichloromethane (see section D, below).

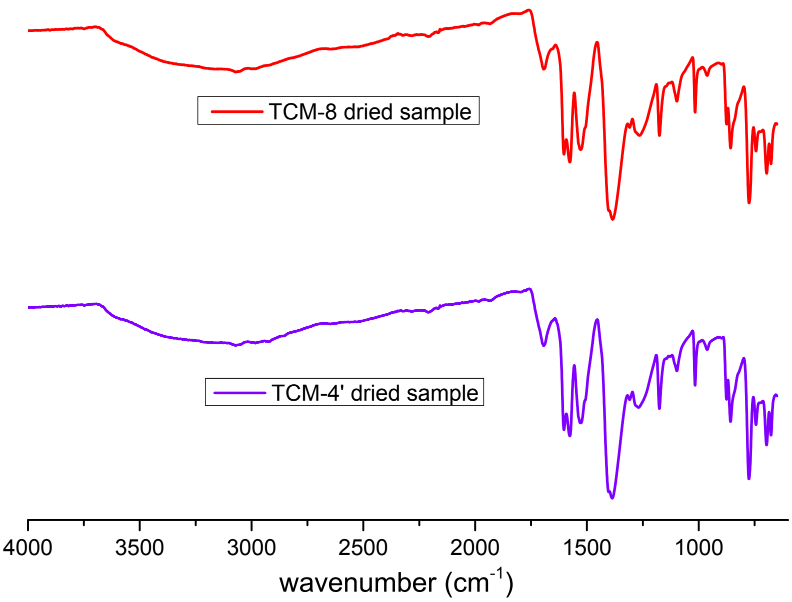

Fig. S1: FT-IR spectra of dried samples of **TCM-4’** and **TCM-8**.

B. Thermogravimeric analysis of TCM-4’ and TCM-8

TGA measurements were carried out using a Perkin-Elmer Pyris-1 analyzer. Crystals were removed from their DMF storage solutions and briefly ‘surface’-dried at room temperature on filter paper (2 minutes) prior to the thermogravimetric analysis. The TGA measurements were carried out under N_2 gas flow (20 ml min^{-1}) between 25˚C and 700˚C. The applied heating rate was 3˚C per minute.

The thermogravimetric analysis of **TCM-4’** is shown in Fig. S2. Upon increasing the temperature to 120˚C, the sample undergoes a weight loss of *ca.* 63% due to the loss of constitutional DMF solvent molecules; the slight weight loss of *ca.* 5% between 120˚C to 260˚C is caused by the loss of coordinated water molecules. The thermogravimetric step above 260˚C can be assigned to the degradation of the BTEB ligand to give a residual sample weight of *ca.* 15% of the original weight above 700˚C. The 63% weight loss due to the removal of DMF solvent molecules correlates to a 74% of the cell volume, which is very close to the void volume (78%) calculated using the crystallographic data (density of the framework 0.413 g/cm^3, density of DMF at room temperature 0.95 g/cm^3).

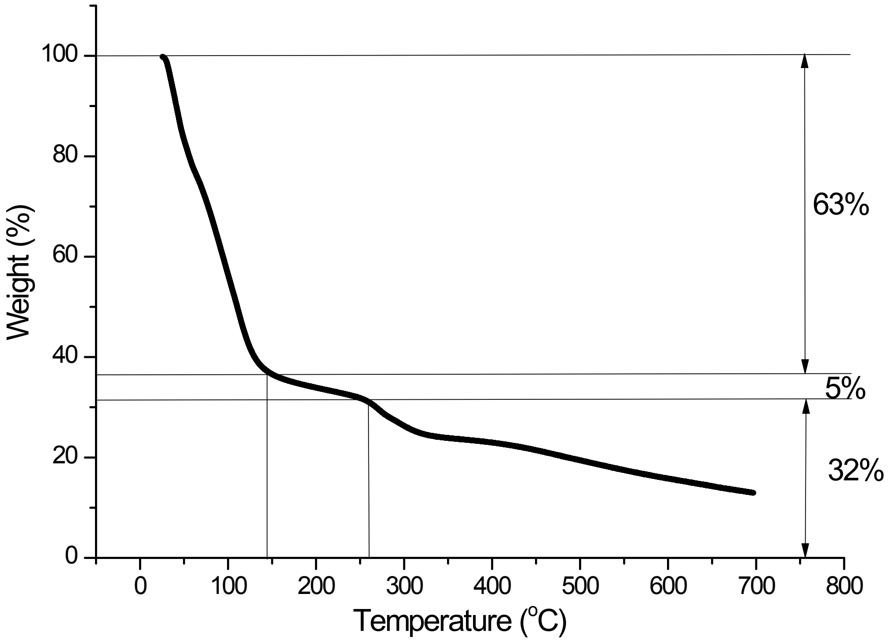

Fig. S2: Thermogravimetric analysis of **TCM-4’** conducted between 25˚C to 700˚C at a heating rate of 3˚C per minute.

The thermogravimetric analysis of **TCM-8** is shown in Fig. S3a. Upon increasing the temperature to 120 ˚C the sample undergoes a weight loss of *ca.* 72%, due to the removal of constitutional DMF solvent molecules. The weight loss of *ca.* 5% between *ca.* 120 ˚C and 280 ˚C can be attributed to the loss of coordinated water molecules. Above 280 ˚C, the organic BTEB ligand undergoes gradually decomposition. The 72% weight loss due to the removal of DMF solvent molecules closely correlates to the void volume (84%) calculated using the crystallographic data (density of the framework 0.317 g/cm^3, density of DMF at room temperature 0.95 g/cm^3). Fig. 3b shows the thermogravimetric analysis of a sample of **TCM-8** where the constitutional solvent molecules were exchanged with dichloromethane (DCM) and which was then dried in vacuum at 30°C.

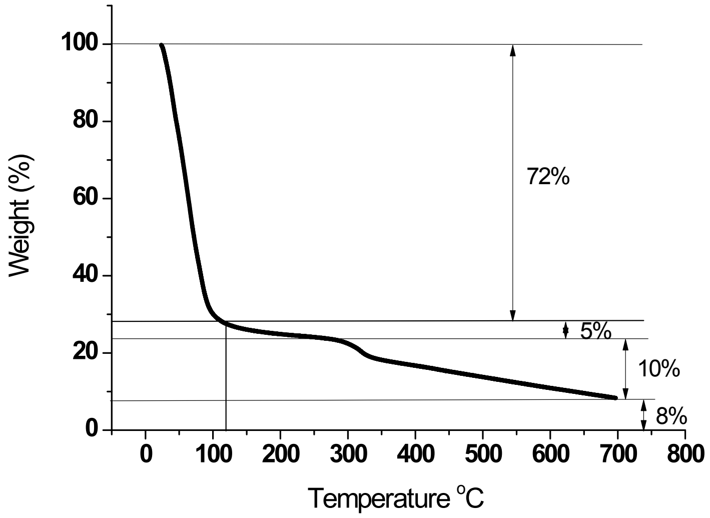

Fig. S3a: Thermogravimetric analysis of **TCM-8** conducted between 25˚C to 700˚C at a heating rate of 3˚C per minute.

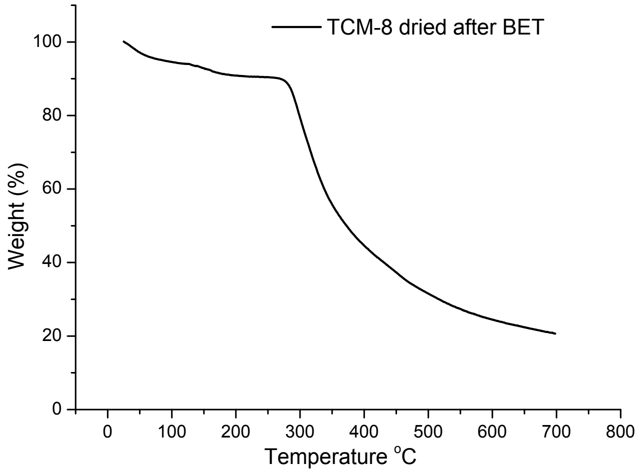

Fig S3b: Thermogravimetric analysis of a dried sample of **TCM-8** (used for BET analysis), heating rate 3ºC/min from 25 ºC to 700 ºC.

C. Crystallographic data.

Single crystals of **TCM-4’** and **TCM-8** were mounted in capillaries containing a small amount of DMF. Data were collected on a Bruker APEX II DUO CCD diffractometer equipped with a Iμ S CuK$_\alpha$ copper microfocus tube (wavelength of 1.54184 Å). The single crystals were cooled to 220(1) K, using an Oxford Cryostream low-temperature device. The diffraction frames were integrated and processed using the Bruker SAINT software package. The data were corrected for absorption effects using the multi-scan method (SADABS).[S1] Space groups were determined using XPREP, and structures were generally solved by Direct Methods (SHELXS) and extended/refined using the SHELXL program.[S2] The positional and anisotropic displacement parameters for the non-hydrogen atoms were refined. Hydrogen atoms were constrained to idealized geometries and allowed to ride on their carrier atoms with an isotropic displacement parameter related to the equivalent displacement parameter of their carrier atoms. All structures contain huge solvent accessible void volumes in which solvent molecules could not be located reliably. To account for this, the Platon-Squeeze routine[S3] was used to calculate the void volumes and re-generate reflections files by excluding the diffraction contributions of these un-located solvent molecules. The final results were based on the new reflection data (results listed in Table S1). Crystal data and numerical details for the data collection and refinement are given in Table S1. Final fractional atomic coordinates, equivalent displacement parameters and anisotropic displacement parameters for the non-hydrogen atoms are given in the cif-files.

Reference:

[S1] Bruker. *SADABS*. **2001**, Bruker AXS Inc., Madison, Wisconsin, USA.

[S2] G. M. Sheldrick, *Acta Cryst.* **2008**, *A64*, 112-122.

[S3] A. L. Spek, *Acta Cryst.* **2009**, *D65*, 148-155.

Table S1. Crystallographic data for **TCM-4'** and **TCM-8**

	TCM-4'	**TCM-8**
Crystal data		
Moiety Formula	$C_{66}H_{36}Cu_3O_{15}$	$C_{66}H_{36}Cu_3O_{15}$
Formula Weight, g.mol^{-1}	1259.57	1259.57
Crystal system	monoclinic	monoclinic
Space group	*C*2/*c*	*C*2/*m*
a, Å	47.493(2)	71.400(8)
b, Å	51.752(2)	42.999(4)
c, Å	32.967(1)	42.569(4)
β, °	92.690(4)	126.08(2)°
V, Å^3	80939(6)	105620(29)
Formula_Z	16	16
Space Group_Z	16	16
ρcalc, g.cm^{-3}	0.413	0.317
F(000), electrons	10224	10224
μ, mm^{-1}	0.532 (Cu Kα)	0.408 (Cu Kα)
Color, habit	blue	blue
Approx. crystal dimension, mm	0.40 x 0.20 x 0.10	0.15 x 0.10 x 0.10
Data collection		
Radiation type; λ, Å	1.54184	1.54184
Temperature, K	220	220
θ range for data collection; min. max., deg	$\theta_{max} = 49.24°$, $\theta_{min} = 1.26°$	$\theta_{max} = 44.64°$, $\theta_{min} = 2.42°$
Index ranges	$-37 \leq h \leq 46$ $-49 \leq k \leq 45$ $-29 \leq l \leq 31$	$-58 \leq h \leq 64$ $-29 \leq k \leq 36$ $-38 \leq l \leq 38$
Max.- Min. absorption transmission factor	0.750 and 0.457	0.749 and 0.059
X-ray exposure time per frame (second)		
Total data	76760	115573
Unique data	34233	39170
Data with criterion: (Fo ≥ 4.0 σ (Fo))	16481	15508
$Rint = \Sigma[\|Fo^2\text{-}Fo^2(\text{mean})\|]/\Sigma[Fo^2]$	0.0826	0.158
Refinement		
Number of reflections	34233	39170
Number of refined parameters	1321	1417
Number of restraints	12	120 (SADI/ISOR etc.)
Final R- index without Platon-squeeze $wR(F2) = [\Sigma[w(Fo^2 - Fc^2)^2] / \Sigma[w(Fo^2)^2]]^{1/2}$ $R(F) = \Sigma (\|\|Fo\| - \|Fc\|\|) / \Sigma \|Fo\|$ For $Fo > 4.0\ \sigma\ (Fo)$	R(F) = 0.207	R(F) = 0.1796
Final R-indexes with Platon-squeeze $wR(F2) = [\Sigma[w(Fo^2 - Fc^2)^2] / \Sigma[w(Fo^2)^2]]^{1/2}$ $R(F) = \Sigma (\|\|Fo\| - \|Fc\|\|) / \Sigma \|Fo\|$ For $Fo > 4.0\ \sigma\ (Fo)$	R(F) = 0.0794, wR(F2) = 0.2018	R(F) = 0.0609, wR(F2) = 0.1273
Weighting scheme: a, b $w = 1/[\sigma^2(Fo^2) + (aP)^2 + bP]$ And $P = [\max(Fo^2,0) + 2Fc^2] / 3$	0.1134 and 0.0	0.0424 and 0.0
$GooF = S = [\ \Sigma\ [w(Fo^2 - Fc^2)^2] / (n\text{-}p)]\ ½$ n = number of reflections p = number of parameters refined	0.901	0.769
Residual electron density in final Difference Fourier map, e/A^3	0.505 and -0.440	0.418 and -0.202 e Å^{-3}
Max. (shift/σ) final cycle	0.001	0.001
Average (shift/σ) final cycle	0.001	0.001
Total Potential Solvent Accessible Void Vol (Å^3) per unit cell, percentage	63340, 78.3%	88500, 83.8%

Crystallographic data, CCDC number 970217 (**TCM-4'**) and 970218 (**TCM-8**), can be obtained free of charge from the Cambridge Crystallographic Data Centre *via* www.ccdc.cam.ac.uk/data_request/cif.

D. Preliminary Surface Area Measurements

Crystals of **TCM-4’** and **TCM-8** were prepared according to the described method. The DMF solvent was removed from the reaction flask using a syringe. Afterwards the crystals were washed with acetone two times and then dispersed in acetone for 3 days. During this period the acetone was refreshed three times. Afterwards the crystals were dispersed in dichloromethane for 3 days. During this period the dichloromethane was exchanged three times. For surface area analyses, ‘wet’ crystals were transferred into a quartz cell using a syringe. Outgassing was performed on the Quantachrome Autosorb IQ at 30˚C for one hour. Then the quartz cell was moved to the measurement station. High-purity helium and nitrogen gases were used for the measurement. **TCM-4’** did not show any permanent porosity due to the limited integrity of the framework structure upon desolvation. **TCM-8** resulted in a Type IV adsorption isotherm with hysteresis effects between P/P_o of 0.8 – 1.0. The determined surface area of **TCM-8** is *ca.* 1020 m^2/g suggesting that the ideal, ordered **tbo** topology is not maintained after the activation procedure. Higher activation temperatures resulted in the loss of the structural integrity of the framework of **TCM-8**.

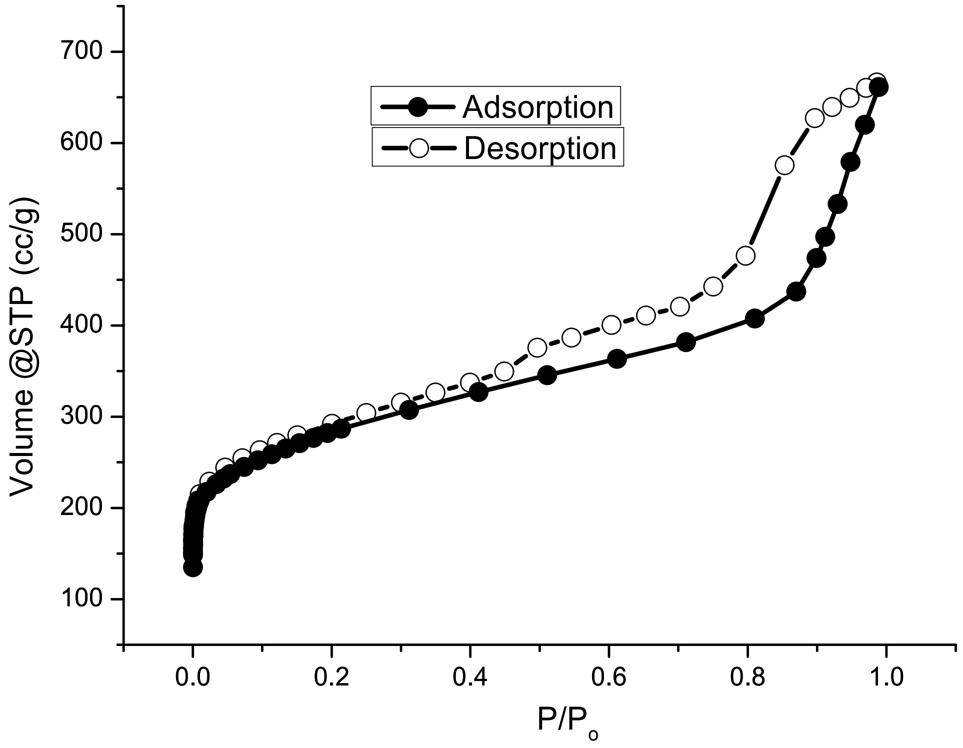

Fig. S4: BET analysis of **TCM-8**. Activated using CH_2Cl_2, dried under vacuum at 160ºC.

E. Powder X-Ray Diffraction Analysis

X-ray powder diffraction patterns were recorded on an APEX II DUO CCD diffractometer equipped with a IμS CuK$_\alpha$ copper source. Micro-crystals were treated with care to avoid the loss of solvent molecules; the samples were generally not exposed to air. To achieve this, manually separated crystals or bulk samples were always kept in DMF solvents. They were ground under solvent to produce micro-crystalline samples and transferred with a pipette into capillaries which were filled 1-2 cm in height. The capillaries were mounted and centered on a Goniometer head on a Bruker APEX II diffractometer for data collection. The data was collected upon 360° ϕ rotational frames at 2θ values of 10° and 20°, with exposure times of 10 or 20 minutes per frame at a detector distance of 120 mm. Overlapping sections of data were combined and the data was processed using the Bruker APEX II routine XRD^2-Eval subprogram. Figs. S5 and S6 show the PXRD patterns of the bulk samples of **TCM-4'** and **TCM-8** and patterns that were calculated based on the single-crystal X-ray diffraction data (using CCDC-Mercury software package). The fit between experimental and calculated patterns confirms the phase-purity of the samples and validates the provided structural models.

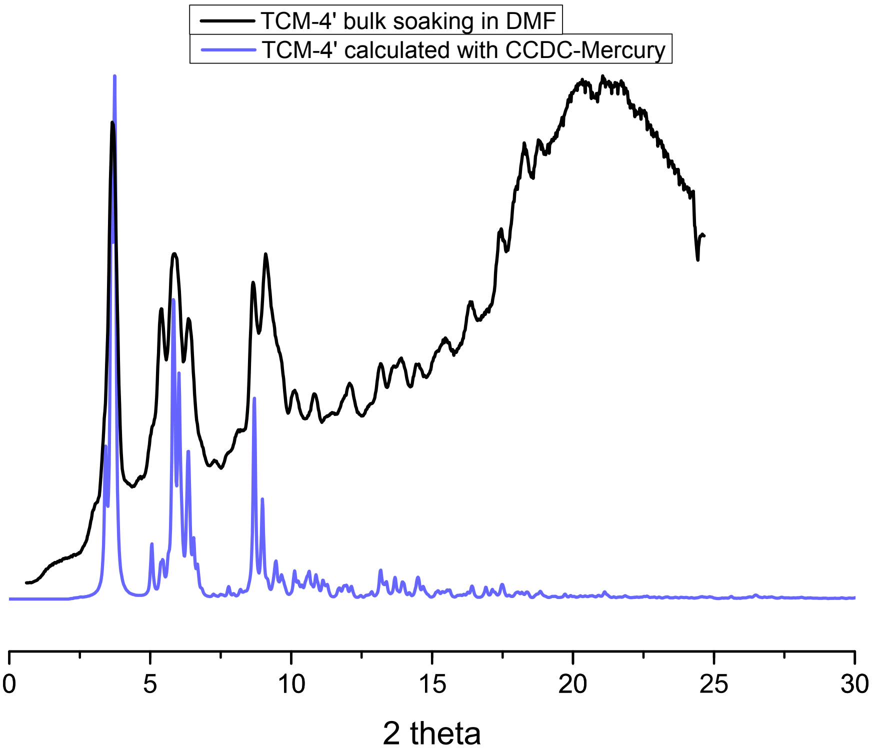

Fig. S5: Powder X-ray diffraction pattern of the bulk sample of **TCM-4'** (black) and its calculated pattern (blue).

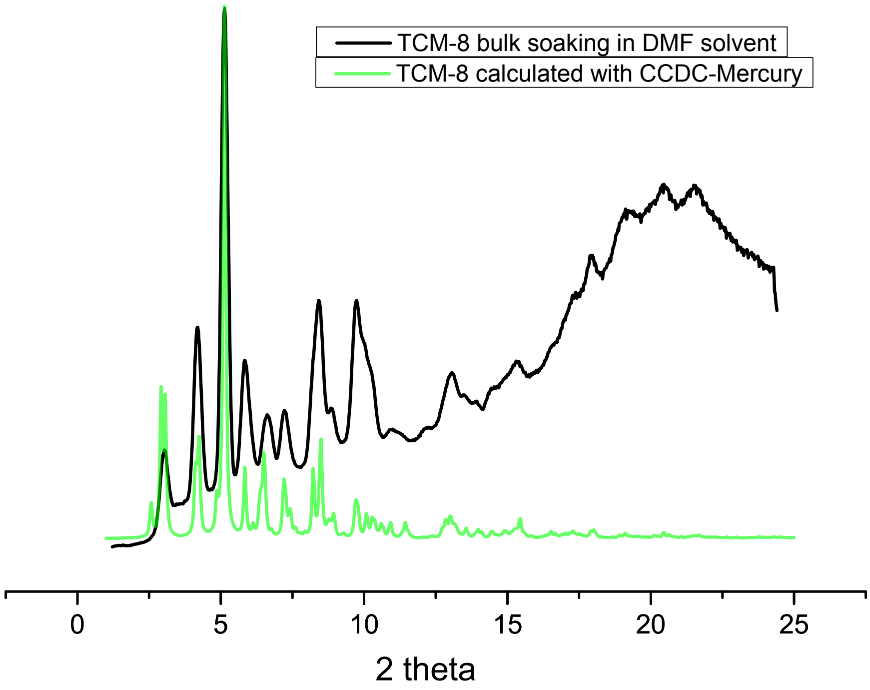

Fig. S6a: Powder X-ray diffraction pattern of the bulk sample of **TCM-8** (black) and its calculated pattern (green).

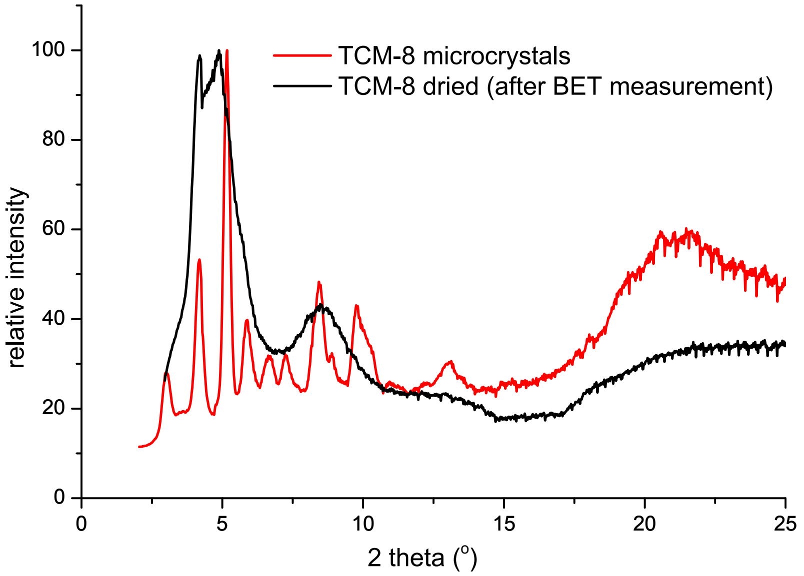

Fig. S6b: Powder X-ray diffraction pattern of a dried sample of **TCM-8** used for BET analysis (black line,) and a solvated microcrystalline sample of **TCM-8** (red line).

E. Simulation Details

The adsorption of nitrogen at 77 K was simulated in **TCM-4’** and **TCM-8** using the grand canonical Monte Carlo (GCMC) method[S4] implemented in the MuSiC software package[S5] using translation, rotation and energy-biased insertion and deletion moves. All simulations were allowed at least 8 x 10^6 equilibration steps, followed by 12 x 10^6 production steps for each pressure point. Both frameworks were treated as rigid, with framework atoms, including those of any coordinated water molecules, kept fixed at their crystallographic positions. The MOFs were considered to be completely activated (no extra-framework molecules such as un-reacted reagents or solvents were included in the simulations) and defect-free. Lennard-Jones parameters for the framework atoms were taken from the DREIDING forcefield[S6] with the exception of copper, for which UFF parameters[S7] were used. Nitrogen was simulated as a rigid molecule using the TraPPE model[S8]. Previous work has shown that nitrogen-MOF electrostatic contributions play only a minor role in nitrogen adsorption[S9] and, as such, only the electrostatic interactions between nitrogen molecules were included in our simulations.

The accessible surface area was calculated by rolling a nitrogen-sized probe sphere (diameter = 3.31 Å) is rolled along the surface of the framework atoms.[S10] The simulated helium pore volume at 298 K was determined using a similar Monte Carlo method, implemented in the Poreblazer tool-set[S11]. The pore size distribution (PSD) of the MOFs was determined using the approach of Gelb and Gubbins[S12] and represents the largest sphere which may be successfully inserted into a particular void space.

References:

[S4] D. Frenkel, Smit, B., *Understanding Molecular Simulation: From Algorithms to Applications*, Academic Press, San Diego, **1996**.

[S5] A. Gupta, S. Chempath, M. J. Sanborn, L. A. Clark, R. Q. Snurr, *Mol. Simul.* **2003**, *29*, 29-46.

[S6] S. L. Mayo, B. D. Olafson, W. A. Goddard, *J Phys Chem-Us* **1990**, *94*, 8897-8909.

[S7] A. K. Rappe, C. J. Casewit, K. S. Colwell, W. A. Goddard, W. M. Skiff, *J. Am. Chem. Soc.* **1992**, *114*, 10024-10035.

[S8] J. J. Potoff, J. I. Siepmann, *Aiche J.* **2001**, *47*, 1676-1682.

[S9] K. S. Walton, R. Q. Snurr, *J. Am. Chem. Soc.* **2007**, *129*, 8552-8556.

[S10] T. Düren, F. Millange, G. Férey, K. S. Walton, R. Q. Snurr, *The Journal of Physical Chemistry C* **2007**, *111*, 15350-15356.

[S11] L. Sarkisov, A. Harrison, *Mol. Simul.* **2011**, *37*, 1248-1257.

[S12] L. D. Gelb, K. E. Gubbins, *Langmuir* **1998**, *14*, 2097-2111.

G. Enlarged Figures

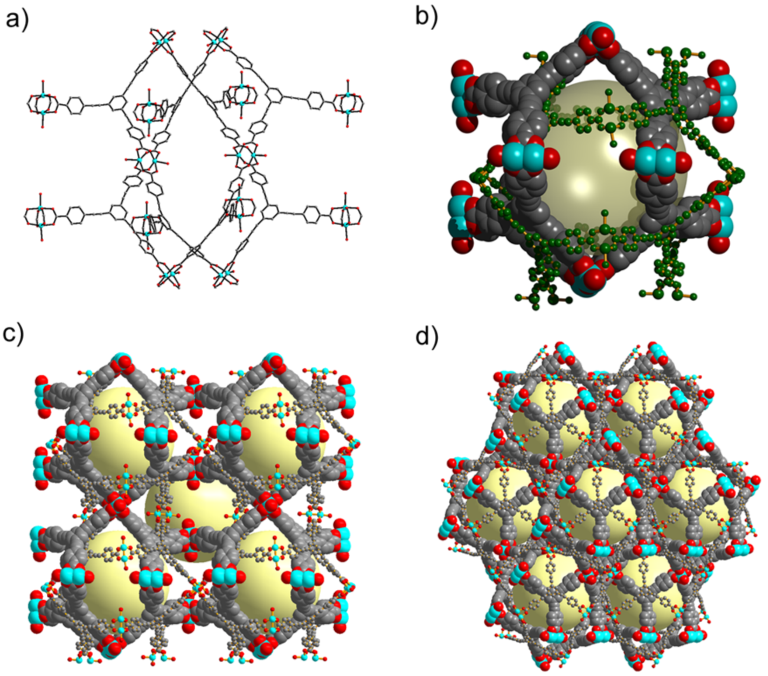

Fig. S7: a) Characteristic structural unit of the **pto**-network in **TCM-4'**; b) Interpenetrated **pto** motifs; c) and d) Packing diagram of the 2-fold interpenetrated **pto**-net with view in the crystallographic [110]- and [101]-directions; largest solvent-accessible void spaces are depicted as yellow spheres whereby the H-atoms and constitutional solvent molecules have been omitted for clarity; colour code Cu cyan, O red, C grey.

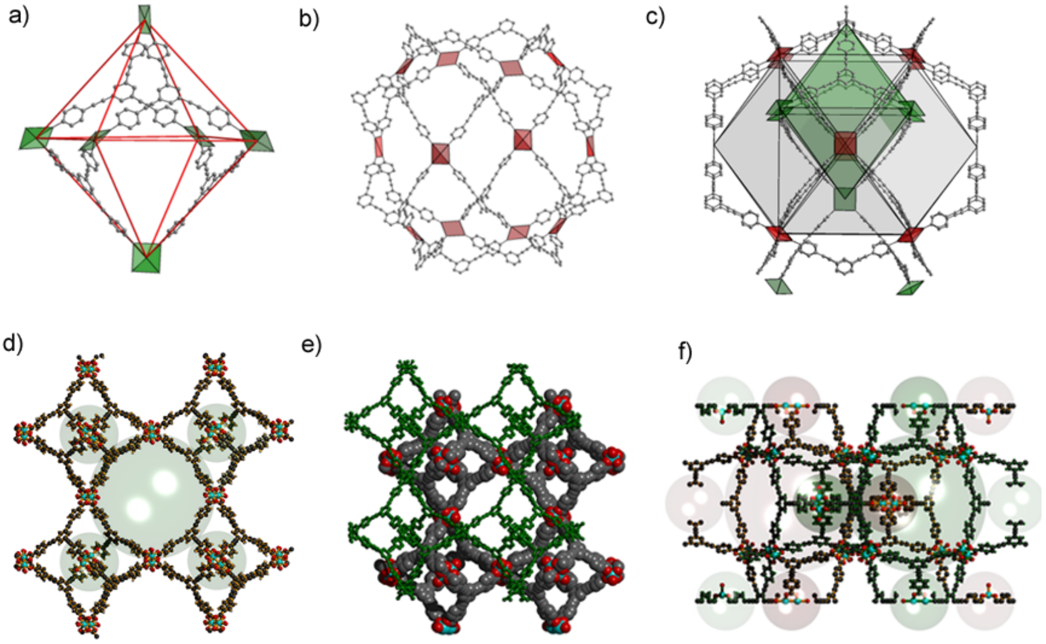

Fig. S8: a) Representation of the octahedral $\{\{Cu_2\}_6(BTEB)_4\}$ cage in **TCM-8**; b) and c) Representation of the cuboctahedral cavity and the interpenetration of octahedral and cuboctahedral cages in **TCM-8**, respectively; d) and e) Structure of **TCM-8**, view in the direction of the crystallographic [101]-direction (single framework d; dual framework e); Representation of the cavities in the dual interpenetrated framework structure of **TCM-8** (cavities that arise from framework I shaded in green whilst those that arise from framework II are shaded in red).